frontiers | Frontiers in Biomaterials Science

TYPE Review
PUBLISHED 10 July 2023
DOI 10.3389/fbiom.2023.1172524

OPEN ACCESS

EDITED BY
Narsimha Mamidi,
Tecnológico de Monterrey, Mexico

REVIEWED BY
Manzar Abbas,
Khalifa University, United Arab Emirates
Pooja Chawla,
Indo-Soviet Friendship College of Pharmacy, India
Aviru Basu,
Institute of Nano Science and Technology (INST), India
Raj Kumar,
University of Nebraska Medical Center, United States

*CORRESPONDENCE
Jianwei Sun,
sjw85985844@163.com

RECEIVED 23 February 2023
ACCEPTED 11 May 2023
PUBLISHED 10 July 2023

CITATION
Gao S, Wang Y, Sun J and Zhang Z (2023), Recent development in black phosphorus nanomaterials for anticancer applications.
Front. Front. Biomater. Sci. 2:1172524.
doi: 10.3389/fbiom.2023.1172524

Recent development in black phosphorus nanomaterials for anticancer applications

Siyang Gao[1], Yuelong Wang[1], Jianwei Sun[1]* and Zhihui Zhang[2]

[1]Chang Chun University of Technology School of Mechatronic Engineering, Changchun, China, [2]Jilin University College of Biological and Agricultural Engineering, Changchun, China

Black phosphorus (BP), also referred to as phosphorene, has gained significant attention in recent years due to its unique structure and properties since its successful exfoliation in 2014. BP's remarkable optical and mechanical properties, electrical conductivity, and electron transfer capabilities position it as a promising alternative to graphene for various biomedical applications. This article provides an overview of the use of BP in cancer imaging, drug delivery, and combination therapy, as well as the challenges and prospects of utilizing BP in practical biomedical applications. While BP shows great potential for biomedical applications, practical implementation remains challenging. Therefore, this review article aims to summarize the latest research on BP and provide insights into its future applications in the biomedical field.

KEYWORDS

cancer, drug delivery, combined treatment, imaging, black phosphorus, two-dimensional materials

1 Introduction

Over the past few years, there has been a tremendous surge in research interest surrounding two-dimensional (2D) materials due to their unique and remarkable properties, such as high surface area to volume ratio, easy functionalization, and remarkable mechanical and electrical properties (Yan et al., 2015; Qin et al., 2020). Among these materials, molybdenum disulfide (MoS2) and other transition metal dichalcogenides (TMDs) have been extensively studied because of their semiconducting properties and atomic-scale thickness (Wang, 2014; Rao et al., 2015). However, MoS2 and other TMDs have limitations in practical applications, such as the relatively low carrier mobility of MoS2. Additionally, while graphene also possesses excellent mechanical and electrical properties, the absence of a bandgap limits its potential applications.

As the growing interest in scientific research illuminates, the potential applications of black phosphorus (BP)-based nano-drug delivery systems are an area of increasing interest (Liu et al., 2021). The unique properties of BP, such as its layer-dependent bandgap, moderate carrier mobility, high capacity of drug loading, intrinsic photothermal and photoacoustic properties, good biocompatibility, and others, make it a highly suitable material for a diverse array of biomedical applications, ranging from phototherapy (photothermal therapy and photodynamic therapy) to drug delivery, bioimaging, and therapeutics and diagnostics. The increasing research interest in this area is a testament to the extraordinary possibilities that BP-based nano-drug delivery systems hold for the future of biomedical research and application (Gao and Mei, 2021). It is worth noting that BP also exhibits outstanding optical performance that positions it as a promising candidate for optoelectronic applications (Sun et al., 2015a). In addition to BP, other 2D materials such as

hexagonal boron nitride (hBN) have been thoroughly investigated due to their potential in nanoelectronics and quantum computing. Specifically, hBN has a wide bandgap and insulating properties, making it an exciting prospect for the development of next-generation electronic devices (Yan and Zhang, 2014; Xu et al., 2016).

Black phosphorus, also called phosphorene, has garnered immense research interest due to its exceptional properties and unique structure since its discovery in 2014 (Mayorga-Martinez et al., 2016). Its monolayer structure features a wrinkled structure in the armchair direction and a bilayer structure in the zigzag direction, resulting in exceptional mechanical, thermoelectric, optical, topological, and electrical conductivity compared to other 2D materials (Jing et al., 2015; Li et al., 2015). While there have been significant strides in understanding BP's nano- and optoelectronic applications, little attention has been paid to its potential biomedical applications. This is mainly due to its instability in air and humid environments (Ezawa, 2014; Wei and Peng, 2014). Recent research, however, has shown the possibility of synthesizing BP in water and air (Fei et al., 2014; Lv et al., 2014; Kumar et al., 2016).

Phosphorus, which is a vital and harmless element and a component of bones, is essential to maintaining human health. As such, BP is a promising and biocompatible material for biomedical applications. Its inherent electrochemical properties have enabled it to be utilized as a biosensing substance to detect target analytes (Zhu et al., 2013; Uk Lee et al., 2015; Zhao et al., 2016). BP, derived from phosphorus, has shown potential as a drug delivery and anti-tumor therapy due to its good biocompatibility, high drug loading efficiency, and photothermal and photodynamic properties (Childers et al., 2011; Childers et al., 2011; Jeong et al., 2011; Comber et al., 2013).

Despite the promising results, there are still technical challenges to overcome in harnessing the full potential of BP in medical applications (Cheng et al., 2012; Sun et al., 2016; Chen et al., 2017a; Chen et al., 2022). However, continued research and development of BP could lead to significant breakthroughs in the biomedical field.

Black phosphorus, or phosphorene, is currently experiencing a surge of interest as a photothermal therapy material thanks to its fascinating properties. It boasts an incredibly high absorption rate and low thermal conductivity, both of which contribute to its unparalleled photothermal and photodynamic efficiency when compared to other metallic materials (Ma et al., 2020). Additionally, the material's high chemical stability renders it a top pick for various biomedical applications, given its ease of biodegradability and the fact that it will not accumulate in the body over time (Kim et al., 2020). This is in contrast to gold materials, which may produce toxic reactions that significantly undermine their efficacy in medical settings (Li et al., 2021).

Peptides, polypeptides, and porphyrin-based systems are also used in photothermal therapy, but their photothermal conversion efficiency is relatively low compared to black phosphorus (Zeng et al., 2020). Additionally, their biocompatibility is not as good as black phosphorus, making it a more attractive option for biomedical applications (Cao et al., 2021; Zhao et al., 2021).

Black phosphorus exhibits exceptional potential for further advancement in the field of photothermal therapy, driven by its remarkable photothermal conversion efficiency and biocompatibility (Jia et al., 2022). Ongoing research and development could potentially revolutionize the landscape of modern healthcare, with black phosphorus serving as a cornerstone of biomedical innovation (Deng et al., 2021).

Black phosphorus (BP) has demonstrated outstanding *in vivo* biodegradability compared to other 2D nanomaterials, making it a safer and highly promising candidate for biomedical applications (Huang et al., 2022). Despite this, the unique advantages of BP over other 2D materials in various biomedical applications have not been clearly summarized (Choi et al., 2018; Nyrop et al., 2022). With the increasing demand for BP in the biomedical field, there is an urgent need to review its applications in fluorescence sensing, colorimetric sensing, electrochemical sensing, and drug delivery (Wang et al., 2022). This review article discusses the applications of BP in cancer imaging, drug delivery, photothermal therapy, and combination therapy. Lastly, the article briefly outlines the challenges and future prospects of BP (Figure 1) (Choi et al., 2018).

2 Application of black scale in cancer imaging

2.1 Optical and electronic properties of black scale

Previous studies have focused on the optical anisotropy of BP (Xia et al., 2014; Mao et al., 2016). Recently, it has been found that BP also exhibits optical anisotropy in the visible region (Çakır et al., 2014; Giaquinto et al., 2022). In addition, Lan et al. (2016) conducted experiments to determine the surface of BP crystals and tuned them by strain engineering. The number of stacked layers also affects the exciton effect and spectrum of BP. Related studies have shown that the luminescence intensity is higher in bilayer BP compared to five-layer BP (Tran et al., 2014; Zhang et al., 2014).

Monolayer BP has high carrier mobility (up to 1,000 cm^2/Vs.) and a direct bandgap that can be adjusted by strain, making it useful for gas detection, including immunosensors and gas sensors for antigen-antibody interaction detection (Anju et al., 2019). BP also exhibits unique electrical properties. Liu et al. (2014) showed that it undergoes a direct-indirect-direct transition in the bandgap under axial pressure, and the bandgap value increases with decreasing layer number. Theoretical studies propose that removing some atoms from the BP monolayer results in blue phosphorene, an indirect semiconductor with a bandgap of ~2 eV (Ospina et al., 2016). Other phosphorus polymorphs with similar stability to BP, such as delta phosphorus (Zhu and Tománek, 2014), g phosphoric acid (Guan et al., 2014a), and beta phosphoric acid (Boulfelfel et al., 2012), also have potential for use in single-layer heterostructures to enable dual (metallic and semiconductor) conduction. These properties make BP a candidate for optoelectronic applications (Guan et al., 2014b; Khandelwal et al., 2017).

2.2 Potential of black phosphorus for photoacoustic cancer imaging

Photoacoustic (PA) imaging is a promising non-invasive technique for cancer imaging that offers high image contrast,

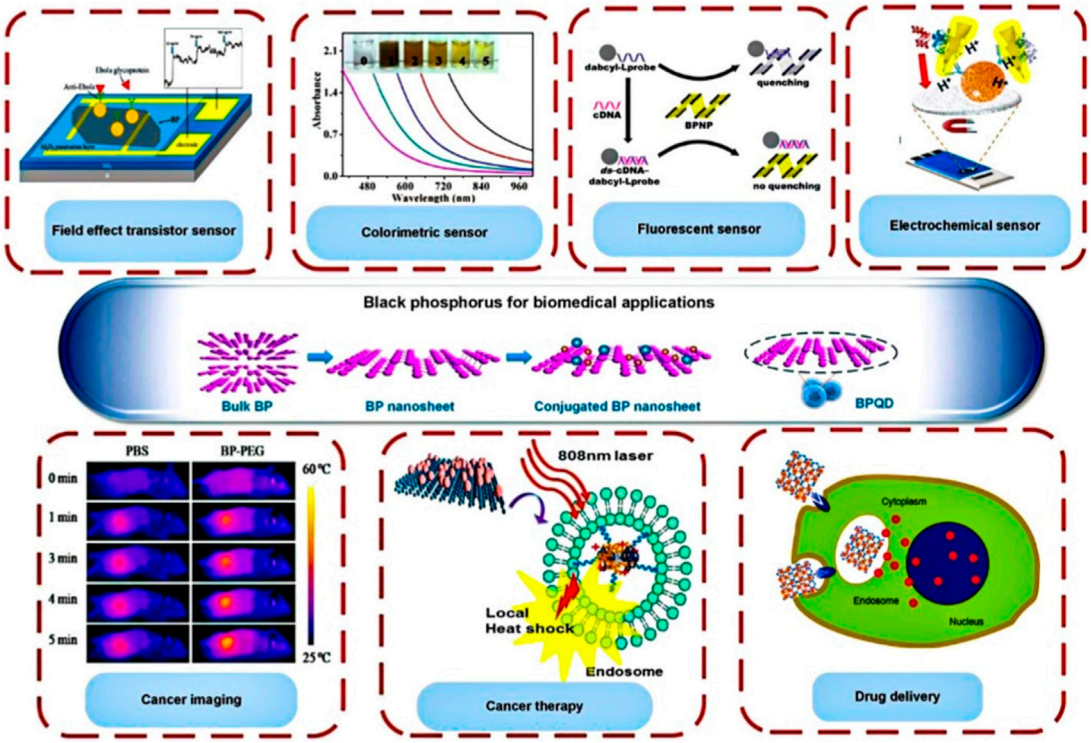

FIGURE 1
Shows the various biomedical applications of BP, including its use as a biosensing material for field-effect transistor sensors, fluorescent sensors, colorimetric sensors, and electrochemical sensors, as well as its applications in cancer imaging, drug delivery, and cancer therapy. BP nanosheets and BP quantum dots (BPQDs) are highlighted as promising materials for these applications (Choi et al., 2018).

sensitivity, and depth-resolved 3D imaging (Kircher et al., 2012; Luke et al., 2012). PA imaging has advantages over other optical imaging techniques, which make it suitable for image-guided therapy (Guo et al., 2022). However, reducing graphene oxide (rGO) using toxic reducing agents may lead to its aggregation, which can affect the bioimaging process. To overcome this, functionalized rGO was introduced to enhance the stability of rGO for biomedical imaging (Mahal et al., 2022).

BP is an attractive material for bioimaging due to its unique optical and electronic properties. It has a tunable bandgap ranging from 0.3 to 2.0 eV for monolayers, making it capable of photodetection in a broad spectral region. Mahal et al. (2022) reported that TiL4-coordinated BPQDs exhibit higher stability and better PA performance in aqueous dispersions than AuNPs due to their larger NIR extinction coefficients (Figures 2A,B). They passively accumulate in tumors due to retention effects and enhanced permeability, showing promise for clinical applications with excellent sensitivity and high spatial resolution in detecting tumors (Figure 2C).

PEGylated boron phosphide nitride phosphides (BPNPs) have been identified as promising candidates for PA imaging and cancer therapy applications owing to their water solubility and stability (Figure 2D). Based on *in vivo* experiments, Sun et al. (2016) found that PEGylated BPNP was retained longer in tumors than in kidneys and livers (Figure 2E), making it a good choice for PA imaging in cancer.

3 Surface modification and drug delivery of black phosphorus

3.1 Surface modification

BP-based nanoparticles have potential for use in modern nanomaterials, but their unique properties limit their biomedical applications. Surface engineering has been used to achieve robust and effective clinical outcomes that overcome these limitations. These approaches demonstrate the multifunctional uses of BP-based nanoparticles in biomedicine.

3.1.1 Modifications using peptides

Although modern nanomaterials have great application potential, their degradability and interactions with biomolecules, such as plasma proteins, limit their biomedical applications. To address this, Wang et al. (2018) synthesized Fmoc-KKF tripeptide for external modification of BP nanosheets, resulting in the stable and long-lasting BP@FKK composite with improved cellular uptake and cytocompatibility. BP has promising applications in photothermal therapy due to its biocompatibility and photothermal properties under near-infrared light, but lacks targeting features and can deteriorate in cancer cells under strong oxidative stress. To overcome these limitations, Zhang et al. (2008) created stable dual-functional BP (DFBP) nanosheets by functionalizing them with mitochondria-targeting peptides and

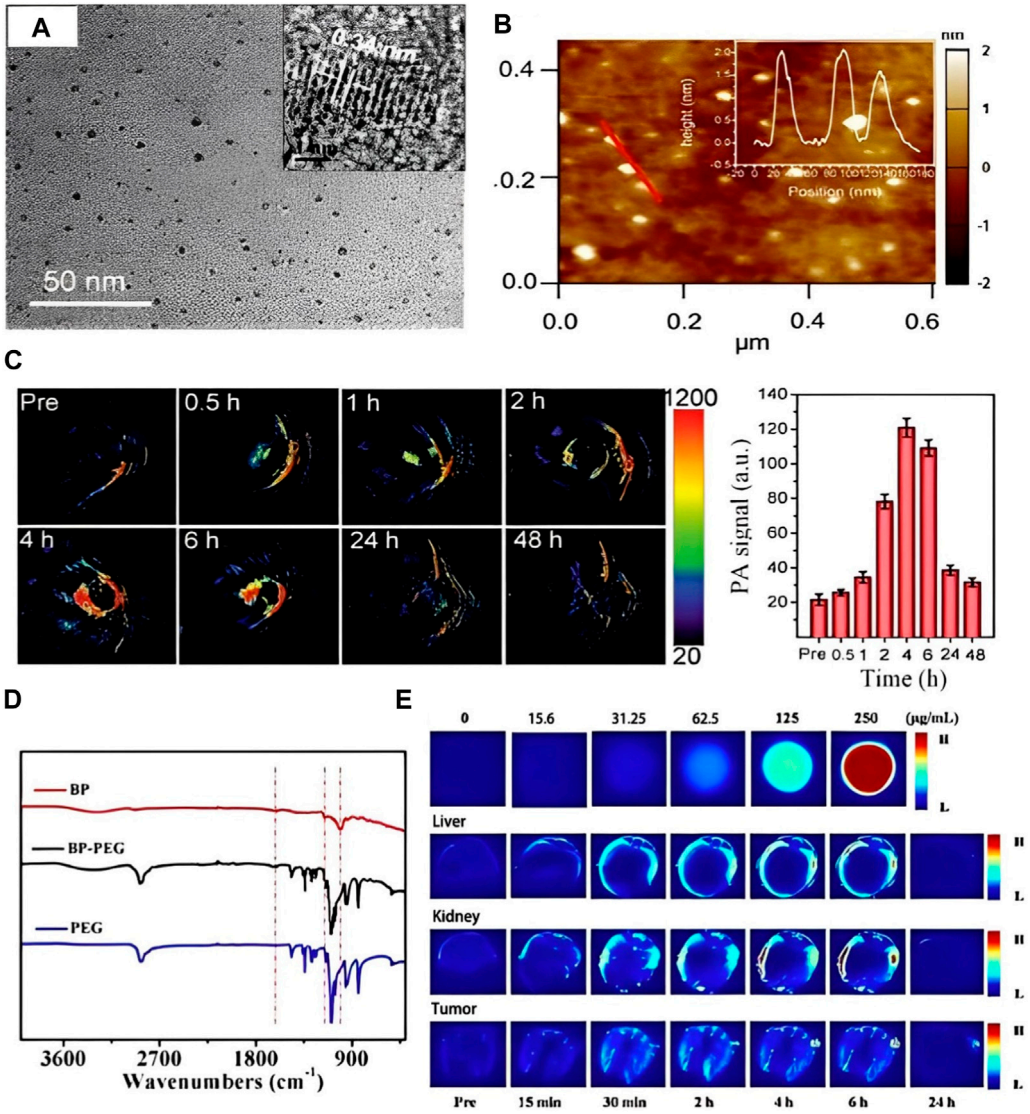

FIGURE 2
Shows **(A)** TEM and **(B)** AFM images of TiL4-coordinated BPQDs. **(C)** Time-dependent PA images and analysis of MCF-7 cells after intravenous injection of TiL4-BPQDs. **(D)** FT-IR spectra of alcoholized BPNP coated with PEG. **(E)** *In vivo* PA images of PEGylated BPNP solution, liver, kidney, and tumor at different time points after injection (Sun et al., 2016).

an acid-labile polymer shell. DFBP nanosheets can be switched to target mitochondria, as shown in Figure 3.

3.1.2 Modification using drugs

BP has unique properties, including high carrier mobility, in-plane anisotropic framework, and a configurable direct bandgap, which make it a promising material for various applications. However, its application is hindered by the easy oxidation of BP to P_xO_y under ambient conditions. To overcome this limitation, a study by Zhang et al. (2019a) used modified cisplatin-Pt-NO3 [Pt$(NH_3)_2(NO_3)_2$] for the surface functionalization of BP nanosheets to produce Pt@BP (Figure 3). This modification allowed Pt@BP to maintain its surface morphology and properties for over 24 h in the environment.

3.1.3 Using polymer modification

BP has poor air stability and insolubility in common organic solvents. Polymer-based nanoparticles can protect guest particles or molecules from degradation and maintain their activity (Lukyanov and Torchilin, 2004). Polymer modulation can neutralize the surface charge, increase the steric impedance between particles, and improve biocompatibility, hydrophilicity, and stability of BP nanomaterials (Friberg, 1984; Sun et al., 2018). Various polymer surface modification methods for BP nanomaterials have been developed (Sun et al., 2015b; Pan et al., 2020).

For instance, BPQDs (BP quantum dots) were fabricated using a liquid exfoliation method combined with an acoustic probe and water bath sonication. After PEG conjugation, BPQDs showed higher stability in physiological media with no obvious toxicity to different types of

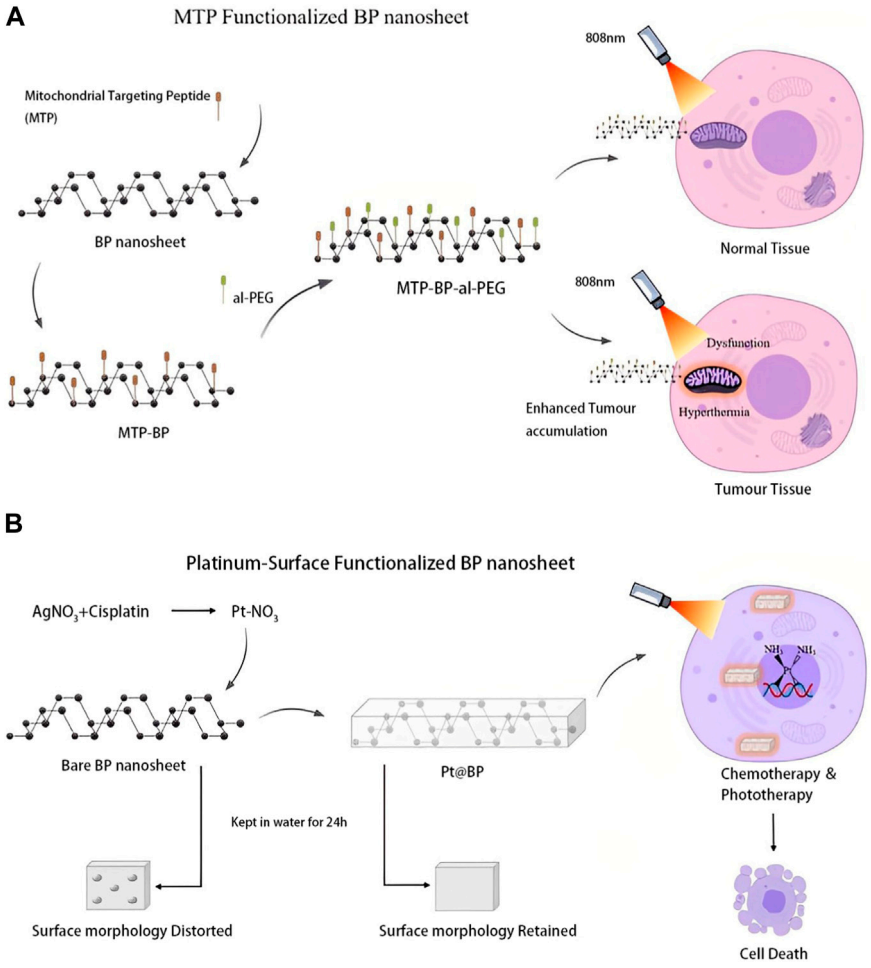

FIGURE 3
Modified cisplatin surface-modified BP nanosheets for synergistic chemotherapy and phototherapy (Zhang et al., 2019b).

cells. Wang et al. (2020a) developed a drug delivery system by functionalizing folic acid moieties linked to PEG-diamine (PEG-NH2-FA) and loading it with an anticancer drug, DOX (doxorubicin). The system, called PEG@BPQD@DOX, was capable of power-photothermal chemotherapy. When NIR (near-infrared) irradiated for 5 min, the temperature of the tumor site rose to 44.2°C. The nanocapsules were configured with a targeting polymer, HS-PEG-FA, and exhibited remarkable photothermal performance, high stability, and the ability to kill cancer cells. DOX was released in the low-pH microenvironment of tumors under NIR laser irradiation, showing a synergistic therapeutic effect by combining photothermal therapy and chemotherapy. For instance, BPQDs (BP quantum dots) were fabricated using a liquid exfoliation method combined with an acoustic probe and water bath sonication. After PEG conjugation, BPQDs showed higher stability in physiological media with no obvious toxicity to different types of cells. Wang et al. (2020b) developed a drug delivery system by functionalizing folic acid moieties linked to PEG-diamine (PEG-NH2-FA) and loading it with an anticancer drug, DOX (doxorubicin). The system, called PEG@BPQD@DOX, was capable of power-photothermal chemotherapy. When NIR (near-infrared) irradiated for 5 min, the temperature of the tumor site rose to 44.2°C. The nanocapsules were configured with a targeting polymer, HS-PEG-FA, and exhibited remarkable photothermal performance, high stability, and the ability to kill cancer cells. DOX was released in the low-pH microenvironment of tumors under NIR laser irradiation, showing a synergistic therapeutic effect by combining photothermal therapy and chemotherapy.

3.1.4 Modification using aptamers and antibodies

Surface modification can enhance the biosensing properties of BP for use in biomedicine. Aptamers can be used for surface modification of BP. For instance, PLL-BP-Apt functionalized Boron Phosphorus Nitrogen Sulfurs (BPNSs) can be used for electrochemical detection of the cardiac biomarker myoglobin. In another study, BP@AuNPs@ aptamer probes combined with immunomagnetic separation were used for electrochemical detection of circulating tumor cells (CTCs) (Figure 4A) (Ma et al., 2022). Liu et al. (2020) utilized BP@AuNPs@ aptamer probes and immunomagnetic separation to detect circulating tumor cells (CTCs) electrochemically. They also developed a biomimetic vesicle using an osteoblast-targeting aptamer linked to PLGA, which guides active targeting of BPQD to cells for biomineralized bone regeneration (Wang et al., 2019). Wang et al.

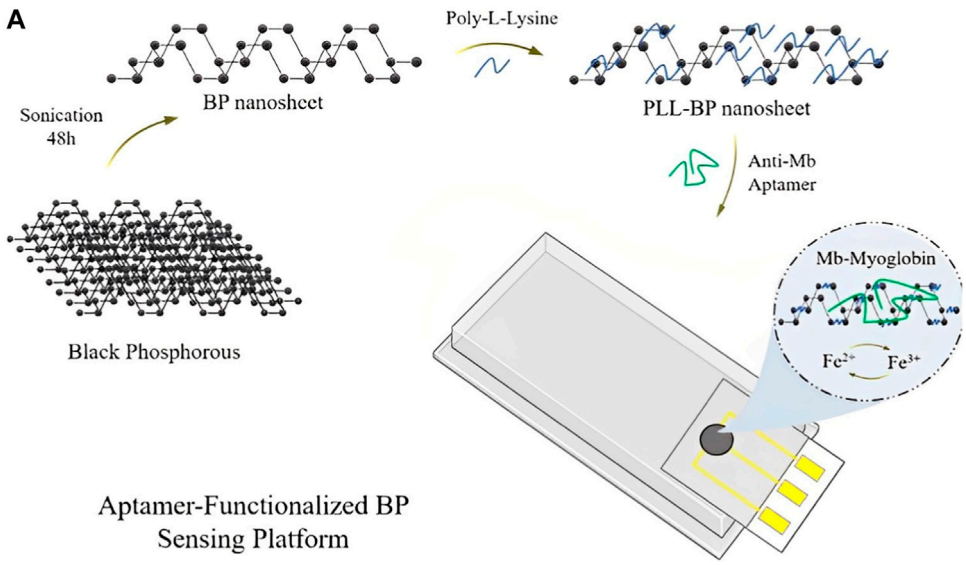

FIGURE 4
Aptamer-functionalized BP sensing platform for yogi globulin detection (Ma et al., 2022).

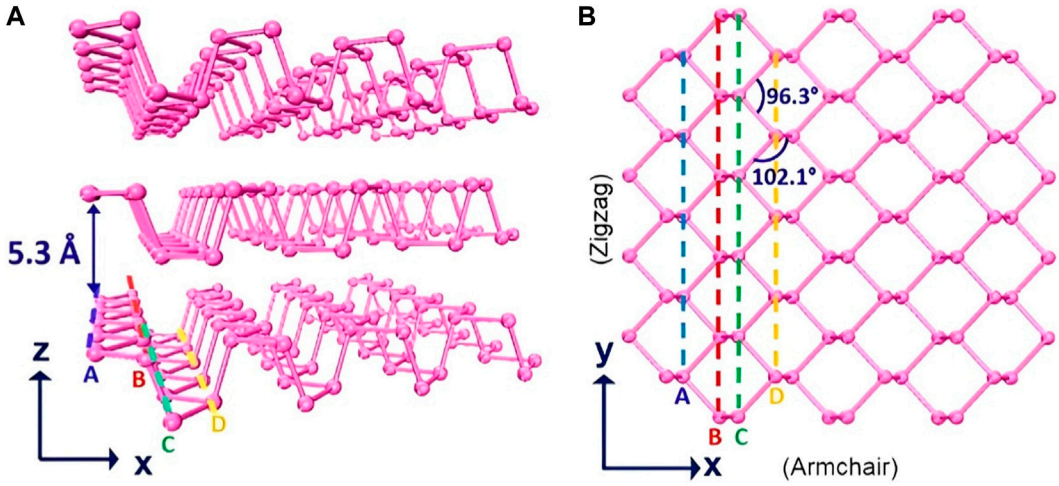

FIGURE 5
Atomic structure of black phosphorus. **(A)** Side view of the black phosphorus crystal lattice. **(B)** Top view of the single-layer black phosphorus lattice (Ling et al., 2015).

(2020a) developed a biomimetic vesicle that guides BPQD to target cells for biomineralized bone regeneration. Additionally, they developed a minimally invasive therapeutic IV catheter for photothermal destruction of CTCs using BP nanosheets modified with anti-EpCAM antibodies. The trapped CTCs are eliminated through downstream mechanisms or the near-infrared-induced photothermal effect of BPNS.

3.1.5 Repair using lipids

Surface modification can improve the biocompatibility of inorganic materials, such as BP, which typically have rough surfaces and sharp edges that can damage cells. Lipid modifications have been shown to enhance intrinsic properties like fluorescence, as demonstrated by BP@lipid-PEG nanospheres with strong NIR-II fluorescence for *in vivo* and *in vitro* imaging (Xu et al., 2019).

3.2 Drug delivery

3.2.1 DDSs construction based on black phosphorus

BP has great potential in drug delivery systems (DDSs) due to its unique properties, including biocompatibility and degradability,

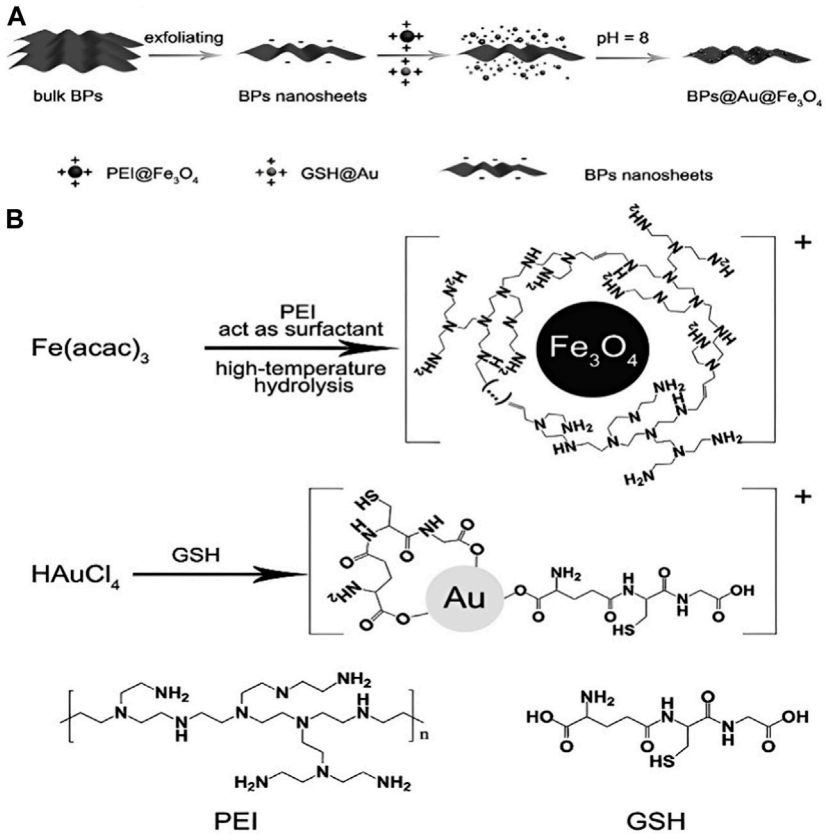

FIGURE 6
(A) Shows the process of creating BPs@Au@Fe3O4 nanoplatform, which involves the deposition of Au and Fe3O4 nanoparticles onto BPNs. Figure 6 **(B)** illustrates the formation of two important precursors used in the process (Yang et al., 2017).

including biocompatibility and degradability, among others (Figure 5) (Ling et al., 2015). BP platforms can be classified into four categories as shown in Figure 5. BP can be used as a carrier for various clinical anticancer drugs, small interfering RNA (siRNA), inorganic components (such as Au, Fe3O4, Pt, and UCNP), and more. BP-based DDSs can be used as carriers for various clinical anticancer drugs, siRNA, inorganic components (such as Au, Fe3O4, Pt, and UCNP), among others. These DDSs can fight cancer through a variety of mechanisms.

Three main strategies have been explored for building BP-based DDSs: electrostatic interactions, non-covalent bonding, and covalent bonding. BP has a negative charge, allowing positively charged drugs to be loaded onto it through electrostatic interactions. Drugs can also be incorporated onto BP delivery platforms through non-covalent bonding or conjugated to them through covalent bonding.

3.2.2 BareBPNs platform

BP's negative charge and corrugated surface structure make it easy to load small, positively charged drugs through electrostatic interaction. In one study (Li et al., 2022), it was found that the electrostatic interaction of BP and DOX resulted in a synergistic combination treatment with a DOX loading capacity of 950 wt%. Methotrexate (MTX), a potent clinical cationic drug, can also be absorbed onto BP nanoparticles (BPNs) through electrostatic interactions and significantly inhibits tumor growth.

Drug delivery systems (DDSs) based on BP nanoparticles (BPNs) have shown great potential as drug delivery substrates, leading to the extension of DDSs based on BPNs to the gene therapy field. Zhou et al. first assembled the Cas9 protein with nuclear localization signals (NLSs) and loaded the resulting Cas9-sgRNA complex onto BPNs through electrostatic interactions to develop a BPN-supported gene therapy platform. The BPN-supported gene therapy platform developed by Zhou et al. demonstrated a loading capacity of 98.7% for the gene-protein carrier system.

BPNs have the advantage of being able to load neutrally or negatively charged drugs after the drugs are electrically modified. The polymer coating strategy is the most effective method to immobilize neutrally or negatively charged drugs on BPNs after these drugs are electrically modified. As shown in Figure 6, Yang et al. modified the surface of BPNs with glutathione (GSH) carboxylic acid groups and PEI, which enabled the effective adsorption of Au NPs and Fe3O4 NPs onto the surface of BPNs (Yang et al., 2017). This modification strategy can be applied to other non-positively charged chemistries, opening up new possibilities for constructing bare BPNs-based DDSs.

In situ reduction is a useful strategy for developing stable BPNs-based DDSs. This strategy does not require additional reducing

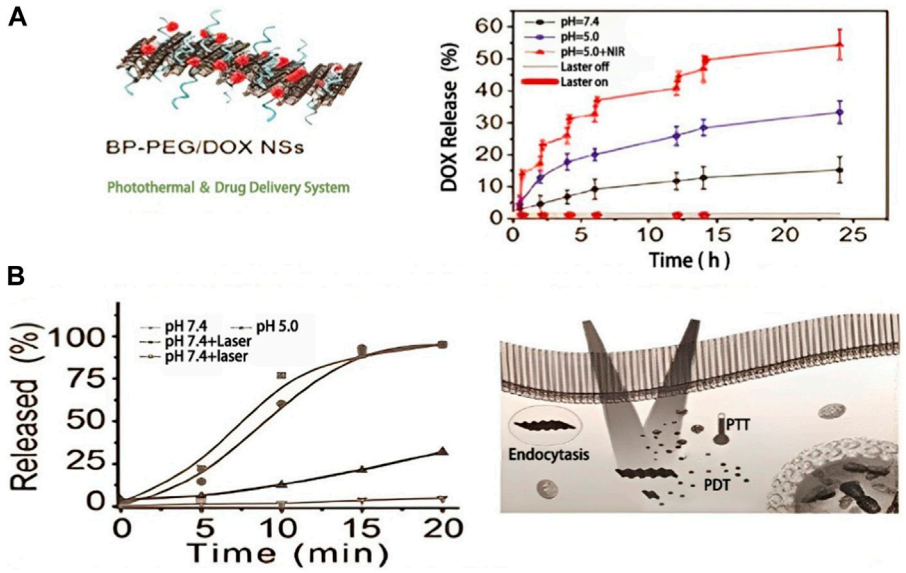

FIGURE 7
Shows drug release kinetics of BP-based DDSs. In **(A)**, BP-PEG/DOX NSs achieved more DOX release at pH 5.0 than at pH 7.4 due to protonation of amino groups on DOX. The release rate at pH 5.0 was 6-fold that at pH 7.4. **(B)** Illustrates DOX release from BP-DOX at pH 5.0 and 7.4 with or without 808 nm irradiation (1 W cm^{-2}) (Chen et al., 2017a).

agents and is based on the good reducing ability of BPNs due to their high Fermi level. In previous studies, Huang et al. (2015) have reported the *in situ* reduction of HAuCl4 on bare BPNs, resulting in uniform spherical AuNPs with an average size of 26 ± 4 nm.

DDSs based on BP can also be constructed using chemical bonds such as covalent, coordinate, and π bonds. For example, Zhao et al. used dinitrogen chemistry to conjugate Nile blue (NB) dye with BP to prepare NB@BP.

3.2.3 Black phosphorus-based stimuli-responsive drug release system

Conventional DDSs suffer from several drawbacks such as immediate and uncontrolled drug release, leading to drug breakdown or denaturation, altered biological distribution, and adverse side effects on healthy tissues and organs. To overcome these issues, smart DDSs have been developed to achieve high-dose and effective continuous therapy while minimizing off-target effects in physiological environments and maximizing tumor therapeutic payloads (Chen et al., 2012).

Smart DDSs are designed to respond to specific stimuli, such as pH, redox potential, enzymatic activation, thermal field, magnetic field, light, ultrasound, and combinations thereof, to achieve controlled drug release. These stimuli take advantage of the differences environments between pathological lesions, tumors, and normal cells. The development of these novel DDSs has great potential in improving the effectiveness and reducing the side effects of anti-tumor therapies.

DDSs based on black phosphorus (BP) have gained attention due to the subtle pH changes in different parts of the human body that can be utilized as stimuli. The pH in the gastrointestinal tract varies from the stomach (pH = 1.0–3.0), small intestine (pH = 6.5–7.0), to colon (pH = 7.0–8.0), while cancer cells have significantly more acidic extracellular pH (pH = 6.5) compared to healthy tissue and blood (pH = 7.5) (Zeng et al., 2015). The four categories that describe how pH affects drug release in BP-based DDSs are drug protonation, coating/capsule breakdown, blood pressure drop, and BP-drug bond disruption.

pH-responsive DDSs can improve the effectiveness of certain anticancer drugs like DOX, which are often limited by their insolubility. Protonating the drug through NH2 in acidic environments can increase its solubility and facilitate its release. In experiments, DDSs achieved significantly more DOX release at pH 5.0 than at pH 7.4, and the release rate at 5.0 was 6 times faster (Figure 7) (Chen et al., 2017b). Similarly, the release rate of the drug MTX increased by about 1.25 times at pH 5.0 due to the protonation of its amino group.

BP-based DDSs can be used for pH-responsive drug release due to the gradual degradation of BP in an acidic environment, leading to the generation of phosphate ions and increased acidity. This mechanism is particularly useful for tumor therapy, as the tumor environment is weakly acidic. Researchers have also investigated the lysosomal escape and siRNA release mechanism of a pH-responsive black phosphorus-based siRNA delivery system (PPBP-siRNA), demonstrating that it can escape from endosomes or early lysosomes (pH = 5.0) into the cytoplasm for gene therapy. This release mechanism is attributed to the degradation of PPBP in an acidic environment, which generates phosphate ions, increases acidity, and promotes endosome swelling, facilitating the release of siRNA. It is worth noting that the generated phosphate ions can also induce calcium phosphate deposition, which can enhance the DDS's biocompatibility and osteogenesis for bone repair.

BP-based DDSs demonstrate sustained drug release triggered by BPN degradation, as shown in Figure 8 (Zhou et al., 2018). Cytosolic release and degradation were studied using fluorescence and Raman intensity mapping. In another study, Shang et al. constructed pH-responsive DDSs based on black phosphorus quantum dots

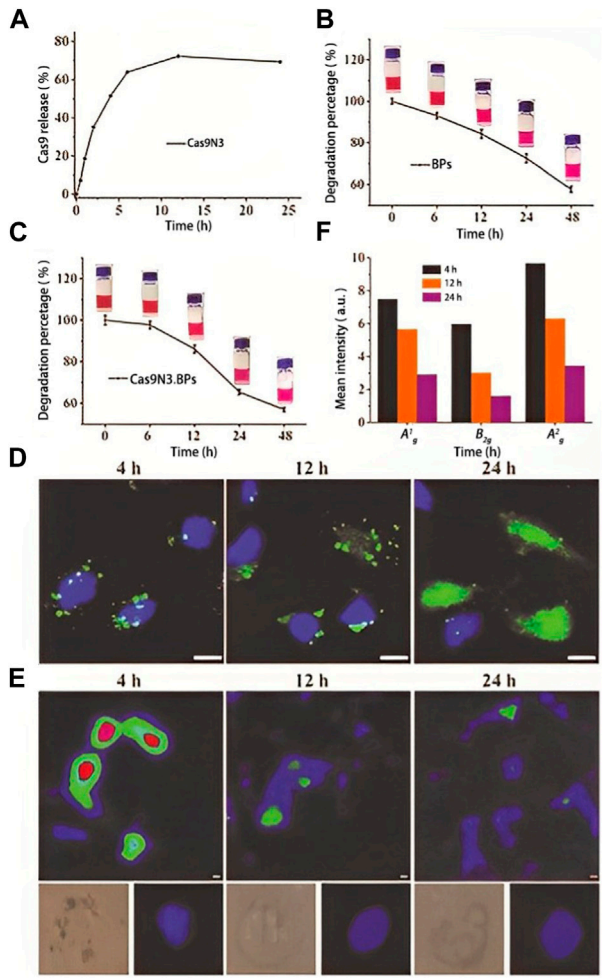

FIGURE 8
Shows the results of a study on the release and degradation of Cas9N3-BPNs for drug delivery. The sustained release of up to 72.2% of Cas9N3 was observed within 12 h, triggered by the degradation of BPNs. Fluorescence and Raman intensity mapping were used to monitor the cytosolic release and degradation of Cas9N3-BPNs in MCF-7 cells. The pH-responsive drug controlled release was demonstrated, with Cas9N3-BPNs degrading more slowly than bare BPNs. The intracellular degradation of BP was monitored using the characteristic A_g^1 Raman peak of BP. The results showed that the release was associated with the biodegradation of BPNs (Zhou et al., 2018).

(BPQDs) camouflaged by platelet membranes. These BPQD-based DDSs exhibited better stability, biocompatibility, and targeting ability compared with traditional DDSs due to the unique properties of platelet membranes.

Coatings or capsules used in BP-based drug delivery systems can be pH dependent, and changes in pH can cause them to break down and result in premature drug release.

PDA is a widely studied coating for BP-based DDSs. It can effectively control drug release and provide continuous tumor therapy. The pH sensitivity of PDA coating allows for dissociation under acidic conditions. Wu et al. showed that drug release in PBS was pH-dependent, with 11.2%, 17.7%, and 31.8% cumulative release at pH 7.4, 6.8, and 5.0, respectively. DOX release was also controlled by the PDA coating, with 13.3% and 29.3% released at pH 7.4 and 5.0, respectively, over 36 h.

PEOz is a polymer with a unique tertiary amide group in the backbone, which can undergo charge reversal at pH values below its pKa, resulting in electrostatic repulsion and accelerated drug release in the slightly acidic microenvironment of tumor cells. DOX release was found to be almost three times higher at pH 5.0 compared to pH 7.4.

To summarize, in the acidic tumor microenvironment, the coating or capsule on BP can partially peel off, leading to faster drug release. pH-sensitive bonds can be used to achieve controlled release. Catechol-BTZ bond's pH sensitivity accelerates the release as the pH drops. The release of DACHPt from BP/DACHPt was only 16.1% at pH 7.4% and 35.4% at pH 5.0. Under acidic conditions, hydrogen ions uptake by BP weakens coordination between DACHPt and BP, leading to accelerated release.

4 BP nanomaterials as potential photosensitizers for PDTs

The size of nanomaterials can affect cellular responses and photothermal capability. BP nanosheets (NSs) with controlled mean size and thickness were obtained by adjusting sonication time and centrifugation speed. Layered Black Phosphorus (L-BP), Metal-doped Black Phosphorus (M-BP), and Sulfur-doped Black Phosphorus Nanocrystals (S-BP NSs) had mean sizes of 394 ± 75 nm, 118 ± 22 and 4.5 ± 0.6 nm, respectively (Figures 9A–C). Larger sizes had better photothermal performance, as seen by the increased solution temperature under NIR laser irradiation (Figures 9D, E). L-BP was more effective than M-BP and S-BP for photothermal ablation of human breast cancer cells (Fu et al., 2017).

BP nanomaterials are typically made using a top-down method to decrease the planar size and layer count, resulting in an increase in bandgap and NIR absorbance decay. Light-trapping ability is a critical factor in photothermal agents, and layered BPs with a narrow bandgap and dense NIR light-trapping are expected to perform well. However, the relationship between size and photothermal performance requires further study.

BP nanomaterials have potential as photosensitizers for Phosphorus-doped Molybdenum Disulfide (PDTs), Wang et al. (2015) have discovered that ultrathin BP nanosheets (with fewer layers) exhibit photodynamic properties when exposed to light, causing excited electrons to generate cytotoxic reactive oxygen species (ROS). This effect has been observed using a 660 nm laser or a xenon lamp with a 600 nm cut-off filter, but higher photon energies may be required for optimal excitation of BP nanomaterials (Zhou et al., 2019; Hu et al., 2020; Kong et al., 2020).

5 Combination therapy with black phosphorus

5.1 Immunostimulatory ability based on thermal ablation of black phosphorus

To investigate the potential of photothermal agents in enhancing tumor immunogenicity (Sun et al., 2017; Zhang

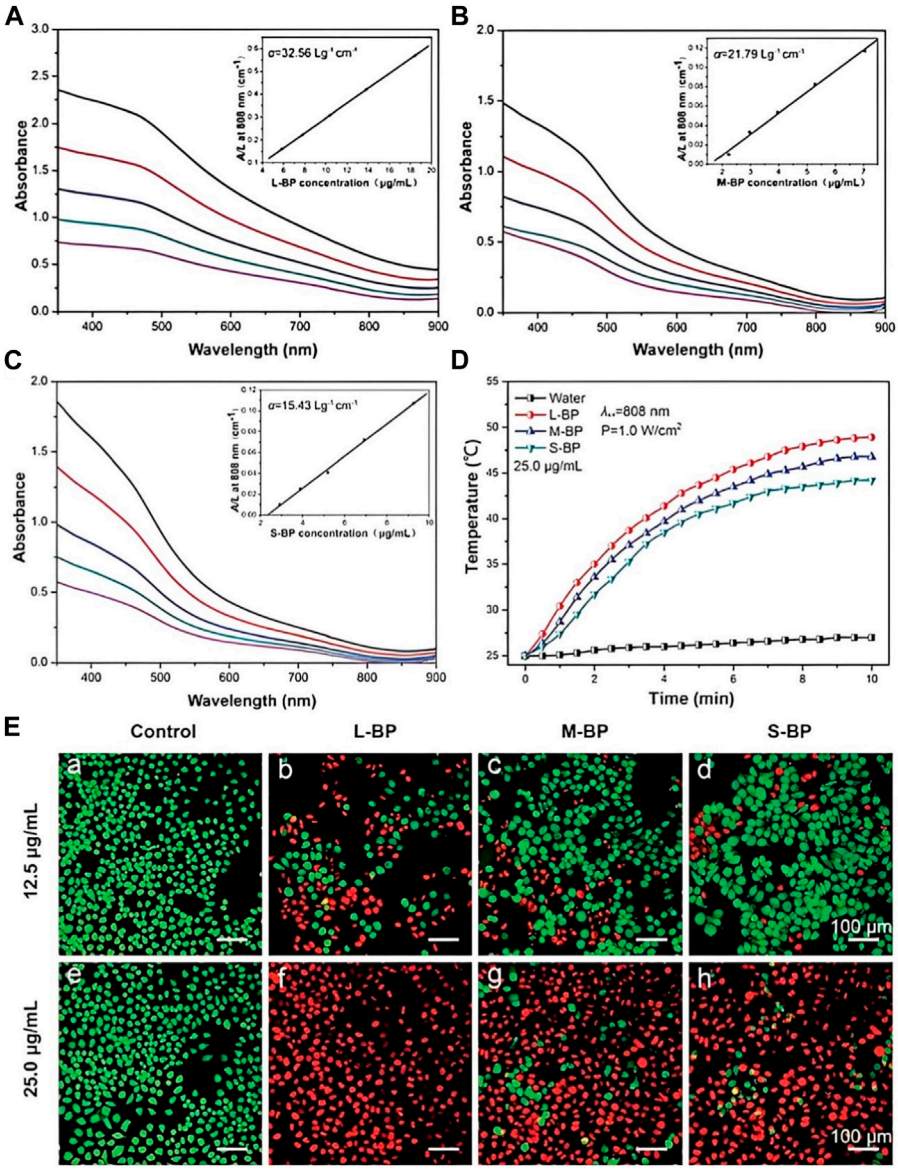

FIGURE 9
Shows the absorbance and photothermal performance of different sized BP nanosheets. The absorbance of L-BP, M-BP, and S-BP in different concentrations of water is presented in panels **(A–C)**, respectively. Panel **(D)** shows the photothermal heating curves of 25.0 μg ml^{-1} L-BP, M-BP, and S-BP aqueous suspensions irradiated by an 808 nm laser for 10 min. Panel **(E)** demonstrates the photothermal ablation of MCF-7 cells incubated with L-BP, M-BP, and S-BP (12.5 and 25.0 μg ml^{-1}) under 808 nm laser (1.0 W cm-2, 15 min) Comparison, where cells were stained with Calcein AM (live cells, green fluorescence) and PI (dead cells, red fluorescence) (Janicke et al., 1998; Zhang et al., 2019b; Zhou et al., 2019).

et al., 2019a; Hu et al., 2020), Xie et al. (2020) evaluated the immune response triggered by photothermal ablation in mice with B-cell lymphoma A20 tumors. The tumor was treated with 20 μg BP and 808-nm NIR laser irradiation for 10 min, resulting in a tumor temperature of ~51 °C, which induced significant cellular necrosis (Figures 10A,B) (Knavel and Brace, 2013). In contrast, tumors treated with PBS and laser irradiation only had a temperature of ~30 °C, causing no tissue damage. The body temperature returned to normal within 3–5 min after laser irradiation. These findings suggest that photothermal ablation using BP can induce cellular necrosis within tumor tissue and has the potential to enhance tumor immunogenicity (Knavel and Brace, 2013).

To investigate the immune response triggered by photothermal therapy using black phosphorus (Chen et al., 2013; Shao et al., 2016; Tao et al., 2017), XIE Z et al. assessed its effects on B-cell lymphoma A20 tumors in mice. After intratumoral exposure to black phosphorus and NIR laser irradiation, cellular necrosis occurred within the tumor tissue, likely due to the development of hypoxia, microvascular thrombosis, and ischemia. Compared to controls, flow cytometry analysis showed an increase in mouse monocytes

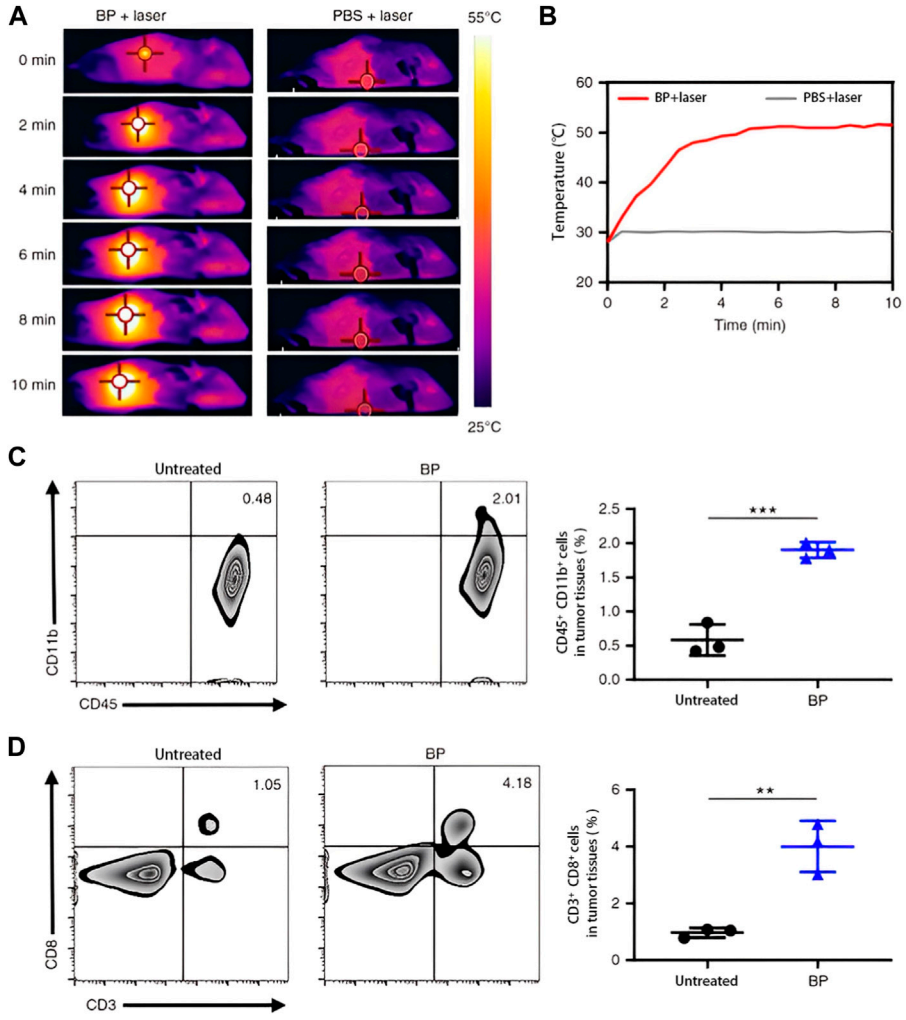

FIGURE 10
BP-based PTT alone ameliorates the immunosuppressive tumor microenvironment. **(A)** Infrared thermal images of A20 tumor-bearing mice exposed to two laser irradiations (808 nm, 1 W cm^{-2}) of BP and PBS. **(B)** 808 nm laser irradiation for 10 min, temperature of the tumor area in BP group and PBS group changed over time. **(C)** Representative graphs of flow cytometry (left) and quantification of $CD45^+$ cells with mouse CD11b+cells (right). **(D)** Representative graphs for flow cytometry (left) and quantification of $CD8^+$ T cells in $CD3^+$ T cells (right) (Knavel and Brace, 2013).

and cytotoxic T lymphocytes in black phosphorus-treated tumors, suggesting the recruitment of more monocytes for phagocytosis of ablated tumor tissue and the promotion of apoptotic death of cancer cells (Figure 10C) (Mildner et al., 2016). These findings indicate the potential of black phosphorus-based photothermal therapy to enhance tumor immunogenicity. Black phosphorus-based photothermal therapy not only destroys tumor cells but also stimulates the immune system by inducing innate and adaptive immune responses (Figure 10D) (Andersen et al., 2006). Thus, black phosphorus-based PTT acts as a potent immunostimulator that can reverse the tumor immunosuppressive microenvironment and promote CTL-mediated antitumor immunity. Therefore, black phosphorus with photothermal effects as specific immunostimulators have great potential for enhancing cancer immunotherapy (Goel et al., 2014; Sun et al., 2015a; Wilhelm et al., 2016).

5.2 Combination of BP-based PTT and aCD47 *in vivo* therapy

Immune checkpoint blockers often have limited effectiveness in treating tumors due to depletion of CTLs in the tumor microenvironment (Pérez-Medina et al., 2016; Hu et al., 2020). However, recent studies have shown that aCD47 antibodies targeting the “do not eat me” signal have promising prospects for tumor immunotherapy (Xie et al., 2020). CD47 is overexpressed in several types of cancers, including acute lymphoblastic leukemia and multiple myeloma. The A20 cell line is a B-cell lymphoma line that requires a large number of cells for subcutaneous implantation, and subcutaneous tumors form after 10 days (Kunitomo et al., 2022). The researchers hypothesized that immunostimulation facilitated by thermal ablation of BP might produce synergistic potentiation with aCD47 checkpoint inhibitors. To test the synergistic antitumor efficacy of BP-based PTT with aCD47, Balb/c mice were

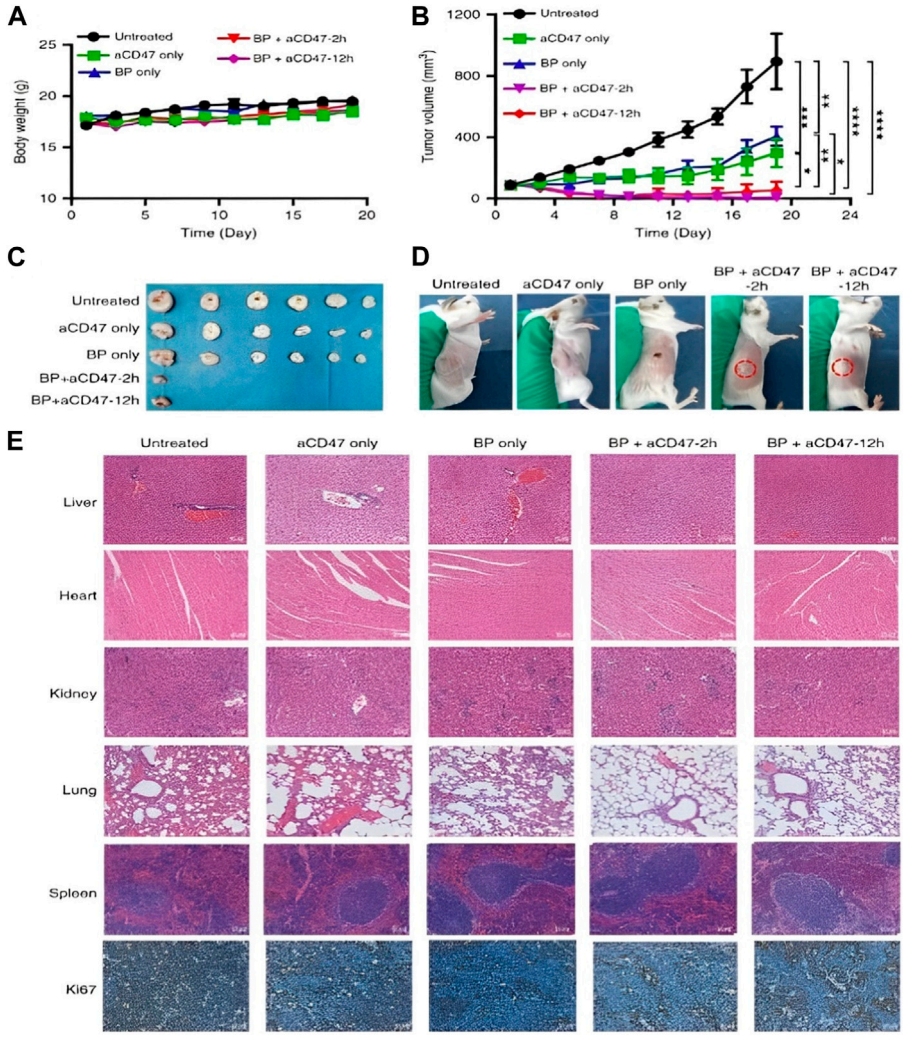

FIGURE 11
Antitumor effect of BP plus aCD47-based PTT treatment. Body weight changes in different mice **(B)** Tumor growth kinetics in different treatment groups. **(C)** Tumors were collected after treatment. **(D)** Shape of mice after treatment (Scholzen and Gerdes, 2000).

subcutaneously inoculated with B-cell lymphoma cells and randomly assigned to five groups (Figure 11A). Combination treatment inhibited tumor growth, as the results show (Figures 11B–D).

Scholzen and Gerdes (2000) conducted a study to investigate the pathological changes caused by various treatments on major organs, including the heart, lungs, liver, spleen, kidney, and tumors in mice. Histopathological analysis was performed on the tissues of the mice. The control group (groups 1, 2, and 3) showed inflammation, congestion, decreased alveolar volume, and alveolar hyperplasia in the lungs, as well as significant liver edema. Combination therapy reduced pathological abnormalities. The expression of Ki-67, a cell marker closely related to proliferation, was significantly reduced in the tumor tissue of the BP + aCD47 combined treatment group, indicating inhibition of cancer cell proliferation and growth. By therapeutic photothermal ablation, the combination of BP and aCD47 inhibited cancer cell proliferation and growth, as confirmed by H&E results (Figure 11E).

5.3 Immune response after BP-PTT + aCD47 blockade

Studies have shown that aCD47 antibodies can convert tumor-specific M2 macrophages into M1-like macrophages, leading to the inhibition of tumor progression (Zhang et al., 2016; Gu et al., 2018). A20 tumor-bearing mice were divided into four groups: Group 1 received no treatment, Group 2 was treated with BP and 808-nm NIR irradiation, Group 3 received aCD47 treatment, and Group 4 received BP and aCD47 treatment. Residual tumor tissues were collected 48 h after treatment, and flow cytometry was used to analyze M1-like macrophages in the tumor tissues. The results showed that the percentage of M1-type macrophage infiltration in the residual tumor was significantly higher in the BP-based PTT and aCD47 combination treatment group compared to the control group, indicating that the combination treatment polarized tumor-specific macrophages into the M1 phenotype (Figure 12A). T cells play a critical role in the immune response against cancer cells, with

10.3389/fbiom.2023.1172524

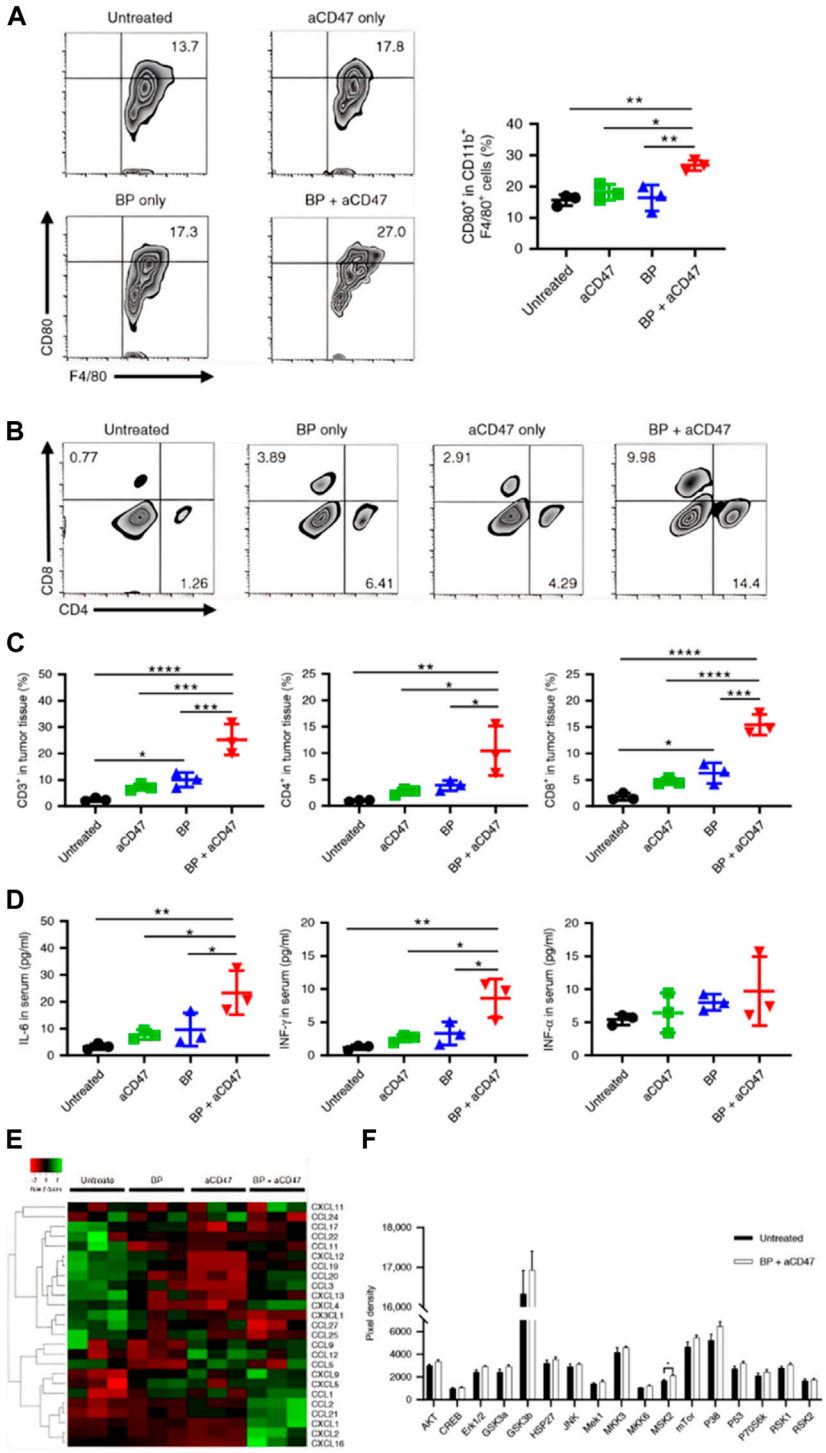

FIGURE 12
BP + aCD47 treatment induces antitumor activity and modulates immune response **(A)** representative flow cytometry result (left) and quantification of CD80$^+$ cells by CD11b$^+$F4/80$^+$ cells (right). **(B)** Representative flow cytometry results of T cell infiltration. **(C)** Percentage of CD8$^+$, CD3$^+$ and CD4$^+$ T cells in tumors after different treatments. **(D)** Cytokine levels in blood isolated from mice on day 5 after different treatments. **(E)** Chemokine levels in mouse tumor isolates 48 h after multiple treatments. **(F)** Quantification of MAPK-phosphorylated proteins in tumors 48 h after treatment (Xie et al., 2020).

CD8$^+$ T cells directly killing cancer cells and CD4$^+$ T cells indirectly regulating the immune response against cancer cells (Gutcher and Becher, 2007; Dillman, 2011; Farhood et al., 2019). To investigate the effect of the combination therapy on tumor-specific T cell responses, different T cell populations in tumors were analyzed after treatment. Furthermore, the proliferation of CD3$^+$ cells was significantly

increased in the BP + aCD47 treatment group, and the number of infiltrating $CD8^+$ and $CD4^+$ cells in tumors was also significantly increased after BP + aCD47 combined treatment compared to controls, indicating the activation of potent adaptive anti-tumor immunity (Figures 12B,C).

Innate and adaptive immune cells secrete cytokines that play important roles in modulating immune responses (Van der Meide and Schellekens, 1996). The results showed that combined treatment with BP and aCD47 increased the secretion of IFN-γ and IL-6, which are key activators of macrophages and stimulate lymphocyte proliferation, respectively (Bhat et al., 2017). This confirmed that the combined treatment promoted innate immune responses as well as CTL-mediated immunity. However, there was no significant increase in TNF-α, which has multiple functions, including tumor promotion, cytotoxicity, and immunomodulation, suggesting that its role in this treatment was unclear (Figure 12D) (Wang and Lin, 2008).

Chemokines are signaling proteins that induce directional chemotaxis in nearby cells and play a crucial role in regulating tumor invasion, proliferation, and metastasis in the tumor microenvironment (Mélik-Parsadaniantz and Rostène, 2008). To further investigate this phenomenon (Nagarsheth et al., 2017), we measured the levels of various chemokines in tumor tissues collected 48 h after treatment using a mouse chemokine array. Notably, CCL21 plays a critical role in initiating T cell responses by attracting dendritic cells and T lymphocytes to the site of inflammation, which enhances the anti-tumor immune response (Figure 12E) (Romagnani et al., 2001; Lin et al., 2014).

The MAPK signaling pathway plays a crucial role in regulating various cellular processes, and its dysregulation can contribute to tumorigenesis (Pearson et al., 2001). To investigate the potential involvement of MAPK signaling in the inhibition of cancer growth induced by the BP + aCD47 combination therapy, tumor tissues were collected 48 h after treatment and analyzed using a MAPK phosphorylation array. Interestingly, the expression levels of mitogens activated downstream of the p38 MAPK pathway and MSK2 were found to be significantly increased compared to controls (Figure 12F). MSK2 is known to regulate the transcription of anti-inflammatory cytokines in macrophages and dendritic cells and promote cell death signaling *via* other pathways (Vermeulen et al., 2009). Furthermore, the combination therapy efficiently induced phagocytosis of tumor cells by M1-like macrophages and enhanced the activity of tumor-associated T cells, thereby overcoming the inherent non-immunogenicity of tumors.

6 Conclusion and prospects

In addition to the challenges related to the production of high-quality BP, there are also challenges associated with the translation of BP-based technologies to clinical settings. The safety and biocompatibility of BP need to be thoroughly investigated to ensure its practical applications in biomedicine. Furthermore, the long-term stability of BP and its interaction with the biological environment should be thoroughly evaluated to guarantee the safety and efficacy of BP-based biomedical applications. In addition to the challenges related to the production of high-quality BP, there are also challenges associated with the translation of BP-based technologies to clinical settings. The safety and biocompatibility of BP need to be thoroughly investigated to ensure its practical applications in biomedicine. Furthermore, the long-term stability of BP and its interaction with the biological environment should be thoroughly evaluated to guarantee the safety and efficacy of BP-based biomedical applications.

Despite these challenges, the potential of BP for biomedical applications is enormous. Its unique properties, such as its tunable bandgap, high carrier mobility, and efficient light absorption, make it a promising candidate for various applications, including imaging, drug delivery, and therapy. BP has already demonstrated its potential in preclinical studies, and there is a growing interest in exploring its applications in clinical settings.

As the field of BP research continues to grow, it is expected that more efficient and safe methods for BP production and functionalization will be developed. The integration of BP with other nanomaterials and biomolecules may further enhance its properties and broaden its biomedical applications. Overall, BP is a promising material that holds great potential for practical applications in biomedicine and has the potential to make significant contributions to the field of cancer diagnosis and treatment.

Author contributions

SG played a leadership role in the research work, responsible for the overall study design and organization. He conducted extensive literature research and data collection on the application fields of black phosphorus, providing in-depth background knowledge and theoretical basis for the article. In addition, SG also wrote the introduction and related technology introduction part of the article. YW made important contributions to the data analysis. YW also wrote the experimental methods and results part of the article, describing in detail the experimental process and key results of the application of black phosphorus in cancer treatment. JS is mainly responsible for the clinical content in this article. JS evaluated the potential efficacy and safety of black phosphorus in clinical treatment and wrote content relevant to clinical practice. ZZ is one of the expert consultants of this paper, and has in-depth research experience in the biological mechanism of black phosphorus and cancer. He provided professional academic guidance and theoretical support for the article. ZZ conducted an in-depth analysis of the molecular mechanism of the interaction between black phosphorus and cancer cells, and wrote content related to the biological mechanism.

Funding

This work is supported by the Jilin Provincial Science and Technology Department project (No: 20230508146RC).

Conflict of interest

The authors declare that the research was conducted in the absence of any commercial or financial relationships that could be construed as a potential conflict of interest.

Publisher's note

References

Andersen, M. H., Schrama, D., thor Straten, P., and Becker, J. C. (2006). Cytotoxic T cells. *J. Investigative Dermatology* 126 (1), 32–41. doi:10.1038/sj.jid.5700001

Anju, S., Ashtami, J., and Mohanan, P. V. (2019). Black phosphorus, a prospective graphene substitute for biomedical applications. *Mater. Sci. Eng. C* 97, 978–993. doi:10.1016/j.msec.2018.12.146

Bhat, P., Leggatt, G., Waterhouse, N., and Frazer, I. H. (2017). Interferon-γ derived from cytotoxic lymphocytes directly enhances their motility and cytotoxicity. *Cell death Dis.* 8 (6), e2836. doi:10.1038/cddis.2017.67

Boulfelfel, S. E., Seifert, G., Grin, Y., and Leoni, S. (2012). Squeezing lone pairs: The A 17 to A 7 pressure-induced phase transition in black phosphorus[J]. *Phys. Rev. B* 85 (1), 014110. doi:10.1103/PhysRevB.85.014110

Çakır, D., Sahin, H., and Peeters, F. M. (2014). Tuning of the electronic and optical properties of single-layer black phosphorus by strain. *Phys. Rev. B* 90 (20), 205421. doi:10.1103/PhysRevB.90.205421

Cao, J., Qi, J., Lin, X., Xiong, Y., He, F., Deng, W., et al. (2021). Biomimetic black phosphorus nanosheet-based drug delivery system for targeted photothermal-chemo cancer therapy. *Front. Bioeng. Biotechnol.* 9, 707208. doi:10.3389/fbioe.2021.707208

Chen, F., Ellison, P. A., Lewis, C. M., Hong, H., Zhang, Y., Shi, S., et al. (2013). Chelator-free synthesis of a dual-modality PET/MRI agent. *Angew. Chem. Int. Ed.* 52 (50), 13319–13323. doi:10.1002/anie.201306306

Chen, L., Chai, S., Liu, K., Ning, N., Gao, J., Liu, Q., et al. (2012). Enhanced epoxy/silica composites mechanical properties by introducing graphene oxide to the interface. *ACS Appl. Mater. interfaces* 4 (8), 4398–4404. doi:10.1021/am3010576

Chen, W. C., Boreta, L., Braunstein, S. E., Rabow, M. W., Kaplan, L. E., Tenenbaum, J. D., et al. (2022). Association of mental health diagnosis with race and all-cause mortality after a cancer diagnosis: Large-scale analysis of electronic health record data. *Cancer* 128 (2), 344–352. doi:10.1002/cncr.33903

Chen, Y., Ouyang, J., Liu, H., Chen, M., Zeng, K., Sheng, J., et al. (2017b). Black phosphorus nanosheet-based drug delivery system for synergistic photodynamic/photothermal/chemotherapy of cancer. *Adv. Mater.* 29 (5), 1603864. doi:10.1002/adma.201603864

Chen, Y., Ren, R., Pu, H., Chang, J., Mao, S., and Chen, J. (2017a). Field-effect transistor biosensors with two-dimensional black phosphorus nanosheets. *Biosens. Bioelectron.* 89, 505–510. doi:10.1016/j.bios.2016.03.059

Cheng, X. Y., Huang, W. J., Hu, S. C., Zhang, H. L., Wang, H., Zhang, J. X., et al. (2012). A global characterization and identification of multifunctional enzymes. *PloS one* 7 (6), e38979. doi:10.1371/journal.pone.0038979

Childers, D. L., Corman, J., Edwards, M., and Elser, J. J. (2011). Sustainability challenges of phosphorus and food: Solutions from closing the human phosphorus cycle. *Bioscience* 61 (2), 117–124. doi:10.1525/bio.2011.61.2.6

Choi, J. R., Yong, K. W., Choi, J. Y., Nilghaz, A., Lin, Y., Xu, J., et al. (2018). Black phosphorus and its biomedical applications. *Theranostics* 8 (4), 1005–1026. doi:10.7150/thno.22573

Comber, S., Gardner, M., Georges, K., Blackwood, D., and Gilmour, D. (2013). Domestic source of phosphorus to sewage treatment works. *Environ. Technol.* 34 (10), 1349–1358. doi:10.1080/09593330.2012.747003

Deng, X., Liu, H., Xu, Y., Chan, L., Xie, J., Xiong, Z., et al. (2021). Designing highly stable ferrous selenide-black phosphorus nanosheets heteronanostructure via P-Se bond for MRI-guided photothermal therapy. *J. Nanobiotechnology* 19 (1), 201–220. doi:10.1186/s12951-021-00905-5

Dillman, R. O. (2011). Cancer immunotherapy. *Cancer biotherapy Radiopharm.* 26 (1), 1–64. doi:10.1089/cbr.2010.0902

Ezawa, M. (2014). Topological origin of quasi-flat edge band in phosphorene. *New J. Phys.* 16 (11), 115004. doi:10.1088/1367-2630/16/11/115004

Farhood, B., Najafi, M., and Mortezaee, K. (2019). CD8 $^{+}$ cytotoxic T lymphocytes in cancer immunotherapy: A review. *J. Cell. physiology* 234 (6), 8509–8521. doi:10.1002/jcp.27782

Fei, R., Faghaninia, A., Soklaski, R., Yan, J. A., Lo, C., and Yang, L. (2014). Enhanced thermoelectric efficiency via orthogonal electrical and thermal conductances in phosphorene. *Nano Lett.* 14 (11), 6393–6399. doi:10.1021/nl502865s

Friberg, S. (1985). Polymeric stabilization of colloidal dispersions. *J. Dispersion Sci. Technol.* 6 (4), 497. doi:10.1016/j.addr.2003

Fu, H., Li, Z., Xie, H., Sun, Z., Wang, B., Huang, H., et al. (2017). Different-sized black phosphorus nanosheets with good cytocompatibility and high photothermal performance. *RSC Adv.* 7 (24), 14618–14624. doi:10.1039/C7RA00160F

Gao, N., and Mei, L. (2021). Black phosphorus-based nano-drug delivery systems for cancer treatment: Opportunities and challenges. *Asian J. Pharm. Sci.* 16 (1), 1–3. doi:10.1016/j.ajps.2020.03.004

Giaquinto, A. N., Miller, K. D., Tossas, K. Y., Winn, R. A., Jemal, A., and Siegel, R. L. (2022). Cancer statistics for African American/black people 2022. *CA a cancer J. Clin.* 72 (3), 202–229. doi:10.3322/caac.21718

Goel, S., Chen, F., Ehlerding, E. B., and Cai, W. (2014). Intrinsically radiolabeled nanoparticles: An emerging paradigm. *Small* 10 (19), 3825–3830. doi:10.1002/smll.201401048

Gu, S., Ni, T., Wang, J., Liu, Y., Fan, Q., Wang, Y., et al. (2018). CD47 blockade inhibits tumor progression through promoting phagocytosis of tumor cells by M2 polarized macrophages in endometrial cancer. *J. Immunol. Res.* 2018, 1–12. doi:10.1155/2018/6156757

Guan, J., Zhu, Z., and Tománek, D. (2014b). Phase coexistence and metal-insulator transition in few-layer phosphorene: A computational study. *Phys. Rev. Lett.* 113 (4), 046804. doi:10.1103/PhysRevLett.113.046804

Guan, J., Zhu, Z., and Tománek, D. (2014a). Tiling phosphorene. *ACS Nano* 8 (12), 12763–12768. doi:10.1021/nn5059248

Guo, L., Guo, Z., Liang, J., Yong, X., Sun, S., Zhang, W., et al. (2022). Quick microwave assembling nitrogen-regulated graphene supported iron nanoparticles for Fischer-Tropsch synthesis. *Chem. Eng. J.* 429, 132063. doi:10.1016/j.cej.2021.132063

Gutcher, I., and Becher, B. (2007). APC-derived cytokines and T cell polarization in autoimmune inflammation. *J. Clin. investigation* 117 (5), 1119–1127. doi:10.1172/JCI31720

Hu, K., Xie, L., Zhang, Y., Hanyu, M., Yang, Z., Nagatsu, K., et al. (2020). Marriage of black phosphorus and Cu2+ as effective photothermal agents for PET-guided combination cancer therapy. *Nat. Commun.* 11 (1), 2778. doi:10.1038/s41467-020-16513-0

Huang, J., Santos, A. C., Tan, Q., Bai, H., Hu, X., Mamidi, N., et al. (2022). Black phosphorous-based biomaterials for bone defect regeneration: A systematic review and meta-analysis. *J. Nanobiotechnology* 20 (1), 522. doi:10.1186/s12951-022-01735-9

Huang, L., Jia, J., Liu, H., Yuan, Y., Zhao, J., Chen, S., et al. (2015). Surface-mediated selective photocatalytic aerobic oxidation reactions on TiO_2 nanofibres. *RSC Adv.* 5 (70), 56820–56831. doi:10.1039/C5RA07518A

Janicke, R. U., Sprengart, M. L., Wati, M. R., and Porter, A. G. (1998). Caspase-3 is required for DNA fragmentation and morphological changes associated with apoptosis. *J. Biol. Chem.* 273 (16), 9357–9360. doi:10.1074/jbc.273.16.9357

Jeong, S. H., Han, J. H., Kim, J. H., Ahn, M. S., Hwang, Y. H., Lee, H. W., et al. (2011). Bax predicts outcome in gastric cancer patients treated with 5-fluorouracil, leucovorin, and oxaliplatin palliative chemotherapy. *Dig. Dis. Sci.* 56, 131–138. doi:10.1007/s10620-010-1280-8

Jia, C., Zhang, F., Lin, J., Feng, L., Wang, T., Feng, Y., et al. (2022). Black phosphorus-Au-thiosugar nanosheets mediated photothermal induced anti-tumor effect enhancement by promoting infiltration of NK cells in hepatocellular carcinoma. *J. nanobiotechnology* 20 (1), 90. doi:10.1186/s12951-022-01286-z

Jing, Y., Tang, Q., He, P., Zhou, Z., and Shen, P. (2015). Small molecules make big differences: Molecular doping effects on electronic and optical properties of phosphorene. *Nanotechnology* 26 (9), 095201. doi:10.1088/0957-4484/26/9/095201

Khandelwal, A., Mani, K., Karigerasi, M. H., and Lahiri, I. (2017). Phosphorene – the two-dimensional black phosphorous: Properties, synthesis and applications. *Mater. Sci. Eng. B* 221, 17–34. doi:10.1016/j.mseb.2017.03.011

Kim, Y. K., Lee, Y., and Shin, K. Y. (2020). Black phosphorus-based smart electrorheological fluid with tailored phase transition and exfoliation. *J. Industrial Eng. Chem.* 90, 333–340. doi:10.1016/j.jiec.2020.07.032

Kircher, M. F., De La Zerda, A., Jokerst, J. V., Zavaleta, C. L., Kempen, P. J., Mittra, E., et al. (2012). A brain tumor molecular imaging strategy using a new triple-modality MRI-photoacoustic-Raman nanoparticle. *Nat. Med.* 18 (5), 829–834. doi:10.1038/nm.2721

Knavel, E. M., and Brace, C. L. (2013). Tumor ablation: Common modalities and general practices. *Tech. Vasc. interventional radiology* 16 (4), 192–200. doi:10.1053/j.tvir.2013.08.002

Kong, N., Ji, X., Wang, J., Sun, X., Chen, G., Fan, T., et al. (2020). ROS-mediated selective killing effect of black phosphorus: Mechanistic understanding and its guidance for safe biomedical applications. *Nano Lett.* 20 (5), 3943–3955. doi:10.1021/acs.nanolett.0c01098

Kumar, V., Brent, J. R., Shorie, M., Kaur, H., Chadha, G., Thomas, A. G., et al. (2016). Nanostructured aptamer-functionalized black phosphorus sensing platform for label-free detection of myoglobin, a cardiovascular disease biomarker. *ACS Appl. Mater. interfaces* 8 (35), 22860–22868. doi:10.1021/acsami.6b06488

Kunitomo, Y., Bade, B., Gunderson, C. G., Akgün, K. M., Brackett, A., Cain, H., et al. (2022). Racial differences in adherence to lung cancer screening follow-up: A systematic review and meta-analysis[J]. *Chest* 161 (1), 266–275. doi:10.1016/j.chest.2021.07.2172

Lan, S., Rodrigues, S., Kang, L., and Cai, W. (2016). Visualizing optical phase anisotropy in black phosphorus. *Acs Photonics* 3 (7), 1176–1181. doi:10.1021/acsphotonics.6b00320

Li, P., Zhang, D., Liu, J., Chang, H., Sun, Y., and Yin, N. (2015). Air-stable black phosphorus devices for ion sensing. *ACS Appl. Mater. interfaces* 7 (44), 24396–24402. doi:10.1021/acsami.5b07712

Li, X., Li, J., and Zhang, X. (2021). Increased prevalence of breast cancer in female patients with lichen sclerosus. *Acta Pharm. Sin.* 84, 178–180. doi:10.1016/j.jaad.2020.04.062

Li, Z., Yu, Y., Zeng, W., Ding, F., Zhang, D., Cheng, W., et al. (2022). Mussel-inspired ligand clicking and ion coordination on 2D black phosphorus for cancer multimodal imaging and therapy. *Small* 18 (26), 2201803. doi:10.1002/smll.202201803

Lin, Y., Sharma, S., and John, M. S. (2014). CCL21 cancer immunotherapy. *Cancers* 6 (2), 1098–1110. doi:10.3390/cancers6021098

Ling, X., Wang, H., Huang, S., Xia, F., and Dresselhaus, M. S. (2015). The renaissance of black phosphorus. *Proc. Natl. Acad. Sci.* 112 (15), 4523–4530. doi:10.1073/pnas.1416581112

Liu, H., Neal, A. T., Zhu, Z., Luo, Z., Xu, X., Tománek, D., et al. (2014). Phosphorene: An unexplored 2D semiconductor with a high hole mobility. *ACS Nano* 8 (4), 4033–4041. doi:10.1021/nn501226z

Liu, S., Luo, J., Jiang, X., Li, X., and Yang, M. (2020). Gold nanoparticle–modified black phosphorus nanosheets with improved stability for detection of circulating tumor cells. *Microchim. Acta* 187, 397–399. doi:10.1007/s00604-020-04367-8

Liu, W., Dong, A., Wang, B., and Zhang, H. (2021). Current advances in black phosphorus-based drug delivery systems for cancer therapy. *Adv. Sci.* 8 (5), 2003033. doi:10.1002/advs.202003033

Luke, G. P., Yeager, D., and Emelianov, S. Y. (2012). Biomedical applications of photoacoustic imaging with exogenous contrast agents. *Ann. Biomed. Eng.* 40, 422–437. doi:10.1007/s10439-011-0449-4

Lukyanov, A. N., and Torchilin, V. P. (2004). Micelles from lipid derivatives of water-soluble polymers as delivery systems for poorly soluble drugs. *Adv. drug Deliv. Rev.* 56 (9), 1273–1289. doi:10.1016/j.addr.2003.12.004

Lv, H. Y., Lu, W. J., Shao, D. F., and Sun, Y. P. (2014). Enhanced thermoelectric performance of phosphorene by strain-induced band convergence. *Phys. Rev. B* 90 (8), 085433. doi:10.1103/PhysRevB.90.085433

Ma, R. Y., Black, A., and Qian, B. Z. (2022). Macrophage diversity in cancer revisited in the era of single-cell omics. *Trends Immunol.* 43, 546–563. doi:10.1016/j.it.2022.04.008

Ma, T., Huang, H., Guo, W., Zhang, C., Chen, Z., Li, S., et al. (2020). Recent progress in black phosphorus sensors. *J. Biomed. Nanotechnol.* 16 (7), 1045–1064. doi:10.1166/jbn.2020.2963

Mahal, B. A., Gerke, T., Awasthi, S., Soule, H. R., Simons, J. W., Miyahira, A., et al. (2022). Prostate cancer racial disparities: A systematic review by the prostate cancer foundation panel. *Eur. Urol. Oncol.* 5 (1), 18–29. doi:10.1016/j.euo.2021.07.006

Mao, N., Tang, J., Xie, L., Wu, J., Han, B., Lin, J., et al. (2016). Optical anisotropy of black phosphorus in the visible regime. *J. Am. Chem. Soc.* 138 (1), 300–305. doi:10.1021/jacs.5b10685

Mayorga-Martinez, C. C., Mohamad Latiff, N., Eng, A. Y. S., Sofer, Z., and Pumera, M. (2016). Black phosphorus nanoparticle labels for immunoassays via hydrogen evolution reaction mediation. *Anal. Chem.* 88 (20), 10074–10079. doi:10.1021/acs.analchem.6b02422

Mélik-Parsadaniantz, S., and Rostène, W. (2008). Chemokines and neuromodulation. *J. Neuroimmunol.* 198 (1-2), 62–68. doi:10.1016/j.jneuroim.2008.04.022

Mildner, A., Marinkovic, G., and Jung, S. (2016). Murine monocytes: Origins, subsets, fates, and functions[J]. *Microbiol. Spectr.* 4 (5), 4. doi:10.1128/microbiolspec.MCHD-0033-2016

Nagarsheth, N., Wicha, M. S., and Zou, W. (2017). Chemokines in the cancer microenvironment and their relevance in cancer immunotherapy. *Nat. Rev. Immunol.* 17 (9), 559–572. doi:10.1038/nri.2017.49

Nyrop, K. A., Damone, E. M., Deal, A. M., Wheeler, S. B., Charlot, M., Reeve, B. B., et al. (2022). Patient-reported treatment toxicity and adverse events in Black and White women receiving chemotherapy for early breast cancer. *Breast Cancer Res. Treat.* 191 (2), 409–422. doi:10.1007/s10549-021-06439-6

Ospina, D. A., Duque, C. A., Correa, J. D., and Suárez Morell, E. (2016). Twisted bilayer blue phosphorene: A direct band gap semiconductor. *Superlattices Microstruct.* 97, 562–568. doi:10.1016/j.spmi.2016.07.027

Pan, W., Dai, C., Li, Y., Yin, Y., Gong, L., Machuki, J. O., et al. (2020). PRP-chitosan thermoresponsive hydrogel combined with black phosphorus nanosheets as injectable biomaterial for biotherapy and phototherapy treatment of rheumatoid arthritis. *Biomaterials* 239, 119851. doi:10.1016/j.biomaterials.2020.119851

Pearson, G., Robinson, F., Beers Gibson, T., Xu, B. e., Karandikar, M., Berman, K., et al. (2001). Mitogen-activated protein (MAP) kinase pathways: Regulation and physiological functions*. *Endocr. Rev.* 22 (2), 153–183. doi:10.1210/edrv.22.2.0428

Pérez-Medina, C., Abdel-Atti, D., Tang, J., Zhao, Y., Fayad, Z. A., Lewis, J. S., et al. (2016). Nanoreporter PET predicts the efficacy of anti-cancer nanotherapy. *Nat. Commun.* 7 (1), 11838. doi:10.1038/ncomms11838

Qin, L., Jiang, S., and He, H. (2020). Functional black phosphorus nanosheets for cancer therapy[J]. *J. Control. Release* 318, 50–66. doi:10.1016/j.jconrel.2019.12.013

Rao, C. N. R., Gopalakrishnan, K., and Maitra, U. (2015). Comparative study of potential applications of graphene, MoS_2, and other two-dimensional materials in energy devices, sensors, and related areas. *ACS Appl. Mater. interfaces* 7 (15), 7809–7832. doi:10.1021/am509096x

Romagnani, P., Annunziato, F., Lasagni, L., Lazzeri, E., Beltrame, C., Francalanci, M., et al. (2001). Cell cycle–dependent expression of CXC chemokine receptor 3 by endothelial cells mediates angiostatic activity. *J. Clin. investigation* 107 (1), 53–63. doi:10.1172/JCI9775

Scholzen, T., and Gerdes, J. (2000). The ki-67 protein: From the known and the unknown[J]. *J. Cell. physiology* 182 (3), 311–322. doi:10.1002/(SICI)1097-4652(200003)182:3<311::AID-JCP1>3.0.CO;2-9

Shao, J., Xie, H., Huang, H., Li, Z., Sun, Z., Xu, Y., et al. (2016). Biodegradable black phosphorus-based nanospheres for *in vivo* photothermal cancer therapy. *Nat. Commun.* 7 (1), 12967. doi:10.1038/ncomms12967

Sun, C., Cai, W., and Chen, X. (2015b). Positron emission tomography imaging using radiolabeled inorganic nanomaterials. *Accounts Chem. Res.* 48 (2), 286–294. doi:10.1021/ar500362y

Sun, C., Wen, L., Zeng, J., Wang, Y., Sun, Q., Deng, L., et al. (2016). One-pot solventless preparation of PEGylated black phosphorus nanoparticles for photoacoustic imaging and photothermal therapy of cancer. *Biomaterials* 91, 81–89. doi:10.1016/j.biomaterials.2016.03.022

Sun, C., Xie, H., Tang, S., Yu, X., Guo, Z., Shao, J., et al. (2015a). Ultrasmall black phosphorus quantum dots: Synthesis and use as photothermal agents. *Angew. Chem. Int. Ed.* 54 (39), 11526–11530. doi:10.1002/anie.201506154

Sun, C., Xu, Y., Deng, L., Zhang, H., Sun, Q., Zhao, C., et al. (2018). Blood circulation, biodistribution, and pharmacokinetics of dextran-modified black phosphorus nanoparticles. *ACS Appl. Bio Mater.* 1 (3), 673–682. doi:10.1021/acsabm.8b00150

Sun, Z., Zhao, Y., Li, Z., Cui, H., Zhou, Y., Li, W., et al. (2017). TiL_4-Coordinated black phosphorus quantum dots as an efficient contrast agent for *in vivo* photoacoustic imaging of cancer. *Small* 13, 1602896. doi:10.1002/smll.201602896

Tao, W., Zhu, X., Yu, X., Zeng, X., Xiao, Q., Zhang, X., et al. (2017). Black phosphorus nanosheets as a robust delivery platform for cancer theranostics. *Adv. Mater.* 29 (1), 1603276. doi:10.1002/adma.201603276

Tran, V., Soklaski, R., Liang, Y., and Yang, L. (2014). Layer-controlled band gap and anisotropic excitons in few-layer black phosphorus. *Phys. Rev. B* 89 (23), 235319. doi:10.1103/PhysRevB.89.235319

Uk Lee, H., Lee, S. C., Won, J., Son, B. C., Choi, S., Kim, Y., et al. (2015). Stable semiconductor black phosphorus (BP)@titanium dioxide (TiO2) hybrid photocatalysts. *Sci. Rep.* 5 (1), 8691. doi:10.1038/srep08691

Van der Meide, P. H., and Schellekens, H. (1996). Cytokines and the immune response. *Biotherapy* 8 (3-4), 243–249. doi:10.1007/BF01877210

Vermeulen, L., Berghe, W. V., Beck, I. M. E., De Bosscher, K., and Haegeman, G. (2009). The versatile role of MSKs in transcriptional regulation. *Trends Biochem. Sci.* 34 (6), 311–318. doi:10.1016/j.tibs.2009.02.007

Wang, H., Hu, K., Li, Z., Wang, C., Yu, M., et al. (2018). Black phosphorus nanosheets passivation using a tripeptide. *Small* 14 (35), 1801701. doi:10.1002/smll.201801701

Wang, H., Yang, X., Shao, W., Chen, S., Xie, J., Zhang, X., et al. (2015). Ultrathin black phosphorus nanosheets for efficient singlet oxygen generation. *J. Am. Chem. Soc.* 137 (35), 11376–11382. doi:10.1021/jacs.5b06025

Wang, J., Ge, C., Liang, W., Yang, Q., Liu, Q., Ma, W., et al. (2020b). *In vivo* enrichment and elimination of circulating tumor cells by using a black phosphorus and antibody functionalized intravenous catheter. *Adv. Sci.* 7 (17), 2000940. doi:10.1002/advs.202000940

Wang, J., Liang, D., Qu, Z., Kislyakov, I. M., Kiselev, V. M., and Liu, J. (2020a). PEGylated-folic acid–modified black phosphorus quantum dots as near-infrared agents for dual-modality imaging-guided selective cancer cell destruction. *Nanophotonics* 9 (8), 2425–2435. doi:10.1515/nanoph-2019-0506

Wang, W., Li, Z., Nie, X., Zeng, W., Zhang, Y., Deng, Y., et al. (2022). pH-sensitive and charge-reversal polymeric nanoplatform enhanced photothermal/photodynamic synergistic therapy for breast cancer. *Front. Bioeng. Biotechnol.*, 10, 836468. doi:10.3389/fbioe.2022.836468

Wang, X. (2014). Chemical stitching. *Nat. Nanotechnol.* 9 (11), 875–876. doi:10.1038/nnano.2014.257

Wang, X., and Lin, Y. (2008). Tumor necrosis factor and cancer, buddies or foes ?[J]. *Acta Pharmacol. Sin.* 29 (11), 1275–1288. doi:10.1111/j.1745-7254.2008.00889.x

Wang, Y., Hu, X., Zhang, L., Zhu, C., Wang, J., Li, Y., et al. (2019). Bioinspired extracellular vesicles embedded with black phosphorus for molecular recognition-guided biomineralization. *Nat. Commun.* 10 (1), 2829. doi:10.1038/s41467-019-10761-5

Wei, Q., and Peng, X. (2014). Superior mechanical flexibility of phosphorene and few-layer black phosphorus. *Appl. Phys. Lett.* 104 (25), 251915. doi:10.1063/1.4885215

Wilhelm, S., Tavares, A. J., Dai, Q., Ohta, S., Audet, J., Dvorak, H. F., et al. (2016). Analysis of nanoparticle delivery to tumours. *Nat. Rev. Mater.* 1 (5), 16014–16112. doi:10.1038/natrevmats.2016.14

Xia, F., Wang, H., and Jia, Y. (2014). Rediscovering black phosphorus as an anisotropic layered material for optoelectronics and electronics. *Nat. Commun.* 5 (1), 4458. doi:10.1038/ncomms5458

Xie, Z., Peng, M., Lu, R., Meng, X., Liang, W., Li, Z., et al. (2020). Black phosphorus-based photothermal therapy with aCD47-mediated immune checkpoint blockade for enhanced cancer immunotherapy. *Light Sci. Appl.* 9 (1), 161. doi:10.1038/s41377-020-00388-3

Xu, Y., Ren, F., Liu, H., Zhang, H., Han, Y., Liu, Z., et al. (2019). Cholesterol-modified black phosphorus nanospheres for the first NIR-II fluorescence bioimaging. *ACS Appl. Mater. interfaces* 11 (24), 21399–21407. doi:10.1021/acsami.9b05825

Xu, Y., Wang, Z., Guo, Z., Huang, H., Xiao, Q., Zhang, H., et al. (2016). Solvothermal synthesis and ultrafast photonics of black phosphorus quantum dots. *Adv. Opt. Mater.* 4 (8), 1223–1229. doi:10.1002/adom.201600214

Yan, Z., Nika, D. L., and Balandin, A. A. (2015). Thermal properties of graphene and few-layer graphene: Applications in electronics[J]. *IET Circuits, Devices Syst.* 9 (1), 4–12. doi:10.1049/iet-cds.2014.0093

Yan, Z. Q., and Zhang, W. (2014). The development of graphene-based devices for cell biology research. *Front. Mater. Sci.* 8, 107–122. doi:10.1007/s11706-014-0228-x

Yang, D., Yang, G., Yang, P., Lv, R., Gai, S., Li, C., et al. (2017). Assembly of Au plasmonic photothermal agent and iron oxide nanoparticles on ultrathin black phosphorus for targeted photothermal and photodynamic cancer therapy. *Adv. Funct. Mater.* 27 (18), 1700371. doi:10.1002/adfm.201700371

Zeng, F., Qin, H., Liu, L., Chang, H., Chen, Q., Wu, L., et al. (2020). Photoacoustic-immune therapy with a multi-purpose black phosphorus-based nanoparticle. *Nano Res.* 13, 3403–3415. doi:10.1007/s12274-020-3028-x

Zeng, J., Du, P., Liu, L., Li, J., Tian, K., Jia, X., et al. (2015). Superparamagnetic reduction/pH/temperature multistimuli-responsive nanoparticles for targeted and controlled antitumor drug delivery. *Mol. Pharm.* 12 (12), 4188–4199. doi:10.1021/acs.molpharmaceut.5b00342

Zhang, F., Tang, M., Chen, L., Li, R., Wang, X., Duan, J., et al. (2008). Simultaneous quantitation of aconitine, mesaconitine, hypaconitine, benzoylaconine, benzoylmesaconine and benzoylhypaconine in human plasma by liquid chromatography–tandem mass spectrometry and pharmacokinetics evaluation of "SHEN-FU" injectable powder. *J. Chromatogr. B* 873 (2), 173–179. doi:10.1016/j.jchromb.2008.08.008

Zhang, J., Ma, Y., Hu, K., Feng, Y., Chen, S., Yang, X., et al. (2019a). Surface coordination of black phosphorus with modified cisplatin. *Bioconjugate Chem.* 30 (6), 1658–1664. doi:10.1021/acs.bioconjchem.9b00128

Zhang, J., Yan, L., Wang, X., Dong, X., Zhou, R., Gu, Z., et al. (2019b). Tumor microenvironment-responsive $Cu_2(OH)PO_4$ Nanocrystals for selective and controllable radiosentization via the X-ray-triggered fenton-like reaction. *Nano Lett.* 19 (3), 1749–1757. doi:10.1021/acs.nanolett.8b04763

Zhang, M., Hutter, G., Kahn, S. A., Azad, T. D., Gholamin, S., Xu, C. Y., et al. (2016). Anti-CD47 treatment stimulates phagocytosis of glioblastoma by M1 and M2 polarized macrophages and promotes M1 polarized macrophages *in vivo*. *PloS one* 11 (4), e0153550. doi:10.1371/journal.pone.0153550

Zhang, S., Yang, J., Xu, R., Wang, F., Li, W., Ghufran, M., et al. (2014). Extraordinary photoluminescence and strong temperature/angle-dependent Raman responses in few-layer phosphorene. *ACS Nano* 8 (9), 9590–9596. doi:10.1021/nn503893j

Zhao, P., Xu, Y., Ji, W., Zhou, S., Li, L., Qiu, L., et al. (2021). Biomimetic black phosphorus quantum dots-based photothermal therapy combined with anti-PD-L1 treatment inhibits recurrence and metastasis in triple-negative breast cancer. *J. Nanobiotechnology* 19 (1), 181–218. doi:10.1186/s12951-021-00932-2

Zhao, Y., Wang, H., Huang, H., Xiao, Q., Xu, Y., Guo, Z., et al. (2016). Surface coordination of black phosphorus for robust air and water stability. *Angew. Chem.* 128 (16), 5087–5091. doi:10.1002/ange.201512038

Zhou, W., Cui, H., Ying, L., and Yu, X. F. (2018). Enhanced cytosolic delivery and release of CRISPR/Cas9 by black phosphorus nanosheets for genome editing. *Angew. Chem.* 130 (32), 10425–10429. doi:10.1002/ange.201806941

Zhou, W., Pan, T., Cui, H., Zhao, Z., Chu, P. K., and Yu, X. (2019). Black phosphorus: Bioactive nanomaterials with inherent and selective chemotherapeutic effects. *Angew. Chem.* 131 (3), 769–774. doi:10.1002/anie.201810878

Zhu, Y. F., Zhang, J., Xu, L., Guo, Y., Wang, X. P., Du, R. G., et al. (2013). Fabrication and photoelectrochemical properties of ZnS/Au/TiO2 nanotube array films. *Phys. Chem. Chem. Phys.* 15 (11), 4041–4048. doi:10.1039/C3CP43572E

Zhu, Z., and Tománek, D. (2014). Semiconducting layered blue phosphorus: A computational study. *Phys. Rev. Lett.* 112 (17), 176802. doi:10.1103/PhysRevLett.112.176802